Bulletin of Electrical Engineering and Informatics
Vol. 10, No. 3, June 2021, pp. 1415∼1422
ISSN: 2302-9285, DOI: 10.11591/eei.v10i3.2719

A new look on CSI imperfection in downlink NOMA systems

Anh-Tu Le, Dinh-Thuan Do
Faculty of Electronics Technology, Industrial University of Ho Chi Minh City, Vietnam

Article Info

Article history:

Received Sep 29, 2020
Revised Feb 4, 2021
Accepted Apr 29, 2021

Keywords:

Ergodic capacity
NOMA
Energy harvesting

ABSTRACT

Observing that cooperative scheme benefits to non-orthogonal multiple access (NOMA) systems, we focus on system performance analysis of downlink. However, spectrum efficiency is still high priority to be addressed in existing systems and hence this paper presents full-duplex enabling in NOMA systems. Other challenge needs be considered related to channel state information (CSI). In particular, we derive closed-form expressions of outage probability for such NOMA systems under the presence of CSI imperfection. Furthermore, to fully exploit practical environment, we provide system model associated with Nakagami-m fading. The Monte-Carlo simulations are conducted to verify the exactness of considered systems.

This is an open access article under the CC BY-SA license.

Corresponding Author:

Dinh-Thuan Do
Faculty of Electronics Technology
Industrial University of Ho Chi Minh City
12 Nguyen Van Bao, Go Vap Dist., Ho Chi Minh City, Vietnam
Email: dodinhthuan@iuh.edu.vn

1. INTRODUCTION

Due to advantages of superior massive connectivity and spectral efficiency, non-orthogonal multiple access (NOMA) has received considerable consideration as the prominent approach for future wireless networks [1], [2]. As promising feature of NOMA, the same radio resources with different power factors based on their channel conditions share for signals from the plurality of users. At the receiving end, the user with poor channel conditions is able to decodes its own message as considering other user's messages as interference. In constrast, the users with better channel conditions need successive interference cancellation (SIC) to aliviate another users' messages and then they decode their own signal [3], [4]. By allocating different levels of power to users, NOMA relying on power domain to permit multiple users to achieve the same non-orthogonal resources [5]-[8]. The users' messages would be detached with the help of SIC. In such, improving connectivity in IoT needs implementation of NOMA technique [9]. In [10] the authors targeted to security-required and the delay-sensitive users on the same non-orthogonal resource to satisfy requirements in IoT employing NOMA. They proved that the proposed system relying on NOMA paradigm is better than the benchmark OMA scheme. The throughput and energy efficiency are studied in the NOMA scenarios to perform a cellular massive IoT in [11]. further improving network connectivity, NOMA can be applied with cognitive radio and millimeter wave networks [12], [13]. In the maner of cooperative scheme, NOMA exhibits some advantages in term of outage probability and further enhance network connectivity [14]-[20].

Basically, the channel Rayleigh fading is conducted in systems introduced in the above-mentioned studies. In general, the dense obstacles and scattering are in the channels between the base station (BS) and the user which follow Rayleigh fading. Since the propagation encounters fewer obstacles and less scattering,

the Nakagami-m distribution is suitable to model the BS-relay links compared with Rayleigh fading. A key factor, channel fading makes a crucial influence on the performance of NOMA systems. In [21], the authors have studied the NOMA system over Nakagami-m fading to highlight outage performance, but the perfect channel estimation is assumed. Actually, the performance is further degraded by imperfect channel estimation. Therefore, it is very challenging to provide an accurate analysis of the NOMA system under joint impacts of imperfect channel state information (CSI) and Nakagami-m fading.

Although the existing works about NOMA have assumed perfect CSI or the order of the instantaneous channel gain at the transmitter side [22]-[25]. However, this assumption is not suitable in some communication scenarios, such as underwater acoustic (UWA) [26] and high-speed railway (HSR) [27] systems, due to the rapidly changing channel and the large feedback delay. Motivated by such analysis, we consider NOMA system in imperfect CSI case.

2. SYSTEM MODEL

In this paper, we assume the base station(S), two user NOMA($U_i, i \in \{1,2\}$) shown in Figure 1. These nodes are equipped single antenna. To improve bandwidth usage efficiency, the user 1 (U_1) works in full-duplex (FD) mode. Channels in link S-U_1, S-U_2, U_1-U_2 are denoted by h_1, h_2 and h_3, respectively. Self-interference channel existing at user U_1 is denoted by g_1. These channels are followed Nakagami-m channel model.

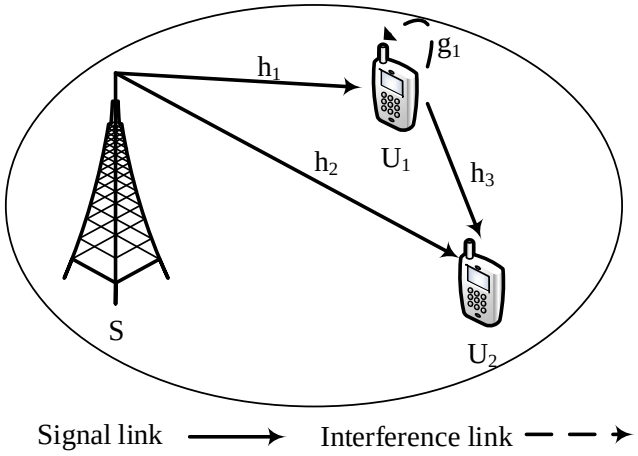

Figure 1. System model

The error channel estimation coefficients is modeled by [28]

$$h_j = \tilde{h}_j + e_j, \tag{1}$$

where $\tilde{h}_j (j \in \{1,2,3\})$ denotes the estimated channel coefficient and e_j denotes the estimated channel error which can be approximated as a Gaussian random variable with $\mathcal{CN}(0, \sigma_j^2)$

In the block time t, the base station S transmits the information $a_1 x_1(t) + a_2 x_2(t)$ to U_i. It is noted that x_1 and x_2 are the information of U_1 and U_2, respectively To proceed NOMA, a_1 and a_2 are the power allocation coefficients where $a_1^2 + a_2^2 = 1$ and $a_1^2 > a_2^2$. Thus, the received signal at U_1 can be computed by

$$\begin{aligned} y_{U_1}(t) &= \sqrt{P_S}\left(a_1 x_1(t) + a_2 x_2(t)\right)\left(\tilde{h}_1 + e_1\right) + \sqrt{P_1} g_1 x_2(t-\tau) + n_1 \\ &= \sqrt{P_S}\tilde{h}_1\left(a_1 x_1(t) + a_2 x_2(t)\right) + \underbrace{\sqrt{P_S} e_1\left(a_1 x_1(t) + a_2 x_2(t)\right) + \sqrt{P_1} g_1 x_2(t-\tau) + n_1}_{\text{effective noise}} \end{aligned} \tag{2}$$

where P_S and P_1 are the power transmission of S and U_1, respectively, n_1 is the additive white Gaussian noise (AWGN) with $\mathcal{CN}(0, N_0)$, g_1 is the residual interference coefficient and τ denotes signal processing delay.

Then, the signal to interference plus noise ratio (SINR) to detect x_2 at U_1 is given by

$$\begin{aligned}\Gamma_{1,2} &= \frac{P_S a_1^2 \left|\tilde{h}_1\right|^2}{P_S a_2^2 \left|\tilde{h}_1\right|^2 + P_S \sigma_1^2 + P_1 \left|g_1\right|^2 + N_0} \\ &= \frac{\rho a_1^2 \left|\tilde{h}_1\right|^2}{\rho a_2^2 \left|\tilde{h}_1\right|^2 + \rho \sigma_1^2 + \rho \left|g_1\right|^2 + 1}\end{aligned} \tag{3}$$

where $\rho = \frac{P_S}{N_0} = \frac{P_1}{N_0}$ is the signal-to-noise ratio (SNR) and the SINR at U_1 to detect the own signal x_1 is given as

$$\Gamma_1 = \frac{\rho a_2^2 \left|\tilde{h}_1\right|^2}{\rho \sigma_1^2 + \rho \left|g_1\right|^2 + 1} \tag{4}$$

Now, the base station S transmits signals to U_2 through two links (direct and relay links). The received signal at U_2 in direct link is expressed as

$$\begin{aligned}y_{U_2}(t) &= \sqrt{P_S}\left(a_1 x_1(t) + a_2 x_2(t)\right)\left(\tilde{h}_2 + e_2\right) + n_2 \\ &= \sqrt{P_S}\tilde{h}_2\left(a_1 x_1(t) + a_2 x_2(t)\right) \underbrace{\sqrt{P_S} e_2 \left(a_1 x_1(t) + a_2 x_2(t)\right) + n_2}_{\text{effective noise}}\end{aligned} \tag{5}$$

It is noted that the signals received at U_2 from U_1 node could be formulated as

$$y_{U_1 \to U_2}(t) = \sqrt{P_1}\left(\tilde{h}_3 + e_3\right) x_2(t-\tau) + n_3 \tag{6}$$

where n_2 and n_3 are the AWGN with $\mathcal{CN}(0, N_0)$.

Then, the SINR to detect x_2 of U_2 is given as

$$\Gamma_2 = \frac{\rho a_1^2 \left|\tilde{h}_2\right|^2}{\rho a_2^2 \left|\tilde{h}_2\right|^2 + \rho \sigma_2^2 + 1}. \tag{7}$$

From (6), the SINR to detect x_2 at U_2 is formulated by

$$\Gamma_{2,1} = \frac{\rho \left|\tilde{h}_3\right|^2}{\rho \sigma_3^2 + 1}. \tag{8}$$

3. PERFORMANCE ANALYSIS

3.1. Channel mode

The probability density function (PDF) of their gains follow gamma distributions is formulated as

$$f_{|h_j|^2}(x) = \frac{x^{m_j - 1} e^{-\frac{m_j}{\Omega_j} x}}{\Gamma(m_j)} \left(\frac{m_j}{\Omega_j}\right)^{m_j}, \tag{9}$$

where m_j and Ω_j are the fading severity factor and mean, respectively.

3.2. Outage probability of U_1

The outage probability of U_1 can be expressed as [29]

$$\mathcal{OP}_{U_1} = 1 - \Pr\left(\Gamma_{1,2} > \gamma_{th2}, \Gamma_1 > \gamma_{th1}\right) \tag{10}$$

where $\gamma_{thi} = 2^{R_i} - 1$ and R_i is the target rate. With the help of (3) and (4), it can be written as

$$\begin{aligned}\mathcal{OP}_{U_1} &= 1 - \Pr\left(\frac{\rho a_1^2 \left|\tilde{h}_1\right|^2}{\rho a_2^2 \left|\tilde{h}_1\right|^2 + \rho\sigma_1^2 + \rho\left|g_1\right|^2 + 1} > \gamma_2, \frac{\rho a_2^2 \left|\tilde{h}_1\right|^2}{\rho\sigma_1^2 + \rho\left|g_1\right|^2 + 1} > \gamma_1\right) \\ &= 1 - \Pr\left(\left|\tilde{h}_1\right|^2 > \frac{\phi\left(\rho\sigma_1^2 + \rho\left|g_1\right|^2 + 1\right)}{\rho}\right)\end{aligned} \tag{11}$$

where $\phi = \max\left(\frac{\gamma_2}{a_1^2 - \gamma_2 a_2^2}, \frac{\gamma_1}{a_2^2}\right)$. Then, (11) is calculated as

$$\mathcal{OP}_{U_1} = 1 - \int_0^\infty f_{|g_1|^2}(x) \int_{\frac{\phi\left(\rho\sigma_1^2 + \rho x + 1\right)}{\rho}}^\infty f_{\left|\tilde{h}_1\right|^2}(y) dy dx \tag{12}$$

Putting (9) into (12), we have

$$\begin{aligned}\mathcal{OP}_{U_1} = 1 &- \frac{1}{\Gamma\left(m_{g_1}\right)\Gamma\left(m_{\tilde{h}_1}\right)}\left(\frac{m_{g_1}}{\Omega_{g_1}}\right)^{m_{g_1}}\left(\frac{m_{\tilde{h}_1}}{\Omega_{\tilde{h}_1}}\right)^{m_{\tilde{h}_1}} \\ &\times \int_0^\infty x^{m_{g_1}-1} e^{-\frac{m_{g_1}}{\Omega_{g_1}}x} \int_{\frac{\phi\left(\rho\sigma_1^2 + \rho x + 1\right)}{\rho}}^\infty y^{m_{\tilde{h}_1}-1} e^{-\frac{m_{\tilde{h}_1}}{\Omega_{\tilde{h}_1}}y} dy dx\end{aligned} \tag{13}$$

Based on [30, Eq. 3.351.2], (13) can be computed as

$$\begin{aligned}\mathcal{OP}_{U_1} = 1 &- \frac{1}{\Gamma\left(m_{g_1}\right)}\left(\frac{m_{g_1}}{\Omega_{g_1}}\right)^{m_{g_1}} e^{-\frac{\phi m_{\tilde{h}_1}\left(\rho\sigma_1^2+1\right)}{\rho\Omega_{\tilde{h}_1}}} \sum_{k=0}^{m_{\tilde{h}_1}-1}\frac{1}{k!}\left(\frac{\phi m_{\tilde{h}_1}\left(\rho\sigma_1^2 + \rho x + 1\right)}{\rho\Omega_{\tilde{h}_1}}\right)^k \\ &\times \int_0^\infty x^{m_{g_1}-1} e^{-\frac{m_{g_1}}{\Omega_{g_1}}x - \frac{\phi m_{\tilde{h}_1}}{\Omega_{\tilde{h}_1}}x} dx\end{aligned} \tag{14}$$

By applying [30, Eq. 1.111], (14) can be further simplified as

$$\begin{aligned}\mathcal{OP}_{U_1} = 1 &- \sum_{k=0}^{m_{\tilde{h}_1}-1}\sum_{n=0}^{k}\binom{k}{n}\frac{\left(\sigma_1^2 + 1/\rho\right)^{k-n}}{k!\Gamma\left(m_{g_1}\right)} e^{-\frac{\phi m_{\tilde{h}_1}\left(\sigma_1^2+1/\rho\right)}{\Omega_{\tilde{h}_1}}}\left(\frac{\phi m_{\tilde{h}_1}}{\Omega_{\tilde{h}_1}}\right)^k\left(\frac{m_{g_1}}{\Omega_{g_1}}\right)^{m_{g_1}} \\ &\times \int_0^\infty x^{m_{g_1}+n-1} e^{-\left(\frac{m_{g_1}\Omega_{\tilde{h}_1} + \phi m_{\tilde{h}_1}\Omega_{g_1}}{\Omega_{g_1}\Omega_{\tilde{h}_1}}\right)x} dx\end{aligned} \tag{15}$$

Finally, using [30, Eq. 3.351.3] the outage probability in closed-form for user U_1 can be obtained as

$$\mathcal{OP}_{U_1} = 1 - e^{-\frac{\phi m_{\tilde{h}_1}\left(\sigma_1^2+1/\rho\right)}{\Omega_{\tilde{h}_1}}} \sum_{k=0}^{m_{\tilde{h}_1}-1}\sum_{n=0}^{k}\binom{k}{n}\frac{\Gamma\left(m_{g_1}+n\right)\left(\sigma_1^2+1/\rho\right)^{k-n}\left(\Omega_{g_1}\right)^n\left(\phi m_{\tilde{h}_1}\right)^k\left(m_{g_1}\right)^{m_{g_1}}}{\Gamma\left(m_{g_1}\right)k!\left(\Omega_{\tilde{h}_1}\right)^{k-m_{g_1}-n}\left(m_{g_1}\Omega_{\tilde{h}_1} + \phi m_{\tilde{h}_1}\Omega_{g_1}\right)^{m_{g_1}+n}} \tag{16}$$

3.3. Outage probability of U_2

In this case, it is assumed that the far user U_2 exploits the selection combine(SC) approach to process two paths achieved from the S and U_1. Thus, the outage probability of U_2 is given as [29]

$$\begin{aligned}\mathcal{OP}_{U_2} &= \Pr\left(\max\left(\Gamma_2, \min\left(\Gamma_{1,2}, \Gamma_{2,1}\right)\right) < \gamma_2\right) \\ &= \underbrace{\Pr\left(\Gamma_2 < \gamma_2\right)}_{A_1}\underbrace{\Pr\left(\min\left(\Gamma_{1,2}, \Gamma_{2,1}\right) < \gamma_2\right)}_{A_2}\end{aligned} \tag{17}$$

Then, putting (7) into the first term of (17), we have

$$\begin{aligned} A_1 &= 1 - \Pr\left(\Gamma_2 > \gamma_2\right) \\ &= 1 - \Pr\left(\left|\tilde{h}_2\right|^2 > \frac{\gamma_2\left(\rho\sigma_2^2+1\right)}{\rho\left(a_1^2-\gamma_2 a_2^2\right)}\right) \\ &= 1 - \int\limits_{\frac{\gamma_2\left(\rho\sigma_2^2+1\right)}{\rho\left(a_1^2-\gamma_2 a_2^2\right)}}^{\infty} f_{\left|\tilde{h}_2\right|^2}(x)dx \end{aligned} \tag{18}$$

Similarly, A_1 is obtained as

$$A_1 = 1 - e^{-\frac{\gamma_2 m_{\tilde{h}_2}\left(\rho\sigma_2^2+1\right)}{\rho\Omega_{\tilde{h}_2}\left(a_1^2-\gamma_2 a_2^2\right)}} \sum_{q=0}^{m_{\tilde{h}_2}-1} \frac{1}{q!}\left(\frac{\gamma_2 m_{\tilde{h}_2}\left(\rho\sigma_2^2+1\right)}{\rho\Omega_{\tilde{h}_2}\left(a_1^2-\gamma_2 a_2^2\right)}\right)^q \tag{19}$$

Furthermore, the second term of (17) is expressed as

$$\begin{aligned} A_2 &= \Pr\left(\min\left(\Gamma_{1,2},\Gamma_{2,1}\right) < \gamma_2\right) \\ &= 1 - \Pr\left(\Gamma_{1,2} > \gamma_2\right)\Pr\left(\Gamma_{2,1} > \gamma_2\right) \end{aligned} \tag{20}$$

Then, we can write $\Pr\left(\Gamma_{1,2} > \gamma_2\right)$ as

$$\begin{aligned} \Pr\left(\Gamma_{1,2} > \gamma_2\right) &= \Pr\left(\left|\tilde{h}_1\right|^2 > \frac{\gamma_2\left(\rho\sigma_1^2+\rho\left|g_1\right|^2+1\right)}{\left(a_1^2-\gamma_2 a_2^2\right)\rho}\right) \\ &= \int\limits_{\frac{\gamma_2\left(\rho\sigma_1^2+\rho|g_1|^2+1\right)}{\left(a_1^2-\gamma_2 a_2^2\right)\rho}}^{\infty} f_{|g_1|^2}(x) \int\limits_{\frac{\gamma_2\left(\rho\sigma_1^2+\rho x+1\right)}{\left(a_1^2-\gamma_2 a_2^2\right)\rho}}^{\infty} f_{\left|\tilde{h}_1\right|^2}(y)dydx \end{aligned} \tag{21}$$

Similar in above, $\Pr\left(\Gamma_{1,2} > \gamma_2\right)$ can be obtained as

$$\begin{aligned} \Pr\left(\Gamma_{1,2} > \gamma_2\right) = 1 - e^{-\frac{\gamma_2 m_{\tilde{h}_1}\left(\sigma_1^2+1/\rho\right)}{\left(a_1^2-\gamma_2 a_2^2\right)\Omega_{\tilde{h}_1}}} \sum_{k=0}^{m_{\tilde{h}_1}-1}\sum_{n=0}^{k}\binom{k}{n} \frac{\Gamma\left(m_{g_1}+n\right)!\left(\sigma_1^2+1/\rho\right)^{k-n}}{\Gamma\left(m_{g_1}\right)k!\left(\Omega_{g_1}\Omega_{\tilde{h}_1}\right)^{-n}\left(m_{g_1}\Omega_{\tilde{h}_1}\right)^{-m_{g_1}}} \\ \times\left(\frac{\gamma_2 m_{\tilde{h}_1}}{\left(a_1^2-\gamma_2 a_2^2\right)\Omega_{\tilde{h}_1}}\right)^k\left(m_{g_1}\Omega_{\tilde{h}_1}+\frac{\gamma_2 m_{\tilde{h}_1}\Omega_{g_1}}{\left(a_1^2-\gamma_2 a_2^2\right)}\right)^{-m_{g_1}-n} \end{aligned} \tag{22}$$

Next, $\Pr\left(\Gamma_{2,1} > \gamma_2\right)$ can be formulated as

$$\Pr\left(\Gamma_{2,1} > \gamma_2\right) = \Pr\left(\left|\tilde{h}_3\right|^2 > \frac{\gamma_2\left(\rho\sigma_3^2+1\right)}{\rho}\right) = \int\limits_{\frac{\gamma_2\left(\rho\sigma_3^2+1\right)}{\rho}}^{\infty} f_{\left|\tilde{h}_3\right|^2}(x)\,dx \tag{23}$$

Similar, after some manipulations, we have

$$\Pr\left(\Gamma_{2,1} > \gamma_2\right) = e^{-\frac{\gamma_2 m_{\tilde{h}_3}\left(\rho\sigma_3^2+1\right)}{\rho\Omega_{\tilde{h}_3}}} \sum_{p=0}^{m_{\tilde{h}_3}-1}\frac{1}{p!}\left(\frac{\gamma_2 m_{\tilde{h}_3}\left(\rho\sigma_3^2+1\right)}{\rho\Omega_{\tilde{h}_3}}\right)^p \tag{24}$$

Putting (22), (23) and (26) into (20) and then with help the result and (19). Finally, the outage probability of U_2 is formulated by

$$\begin{aligned}\mathcal{OP}_{U_2} = &\left(1-e^{-\frac{\gamma_2 m_{\tilde{h}_2}\left(\rho\sigma_2^2+1\right)}{\rho\Omega_{\tilde{h}_2}\left(a_1^2-\gamma_2 a_2^2\right)}}\sum_{q=0}^{m_{\tilde{h}_2}-1}\frac{1}{q!}\left(\frac{\gamma_2 m_{\tilde{h}_2}\left(\rho\sigma_2^2+1\right)}{\rho\Omega_{\tilde{h}_2}\left(a_1^2-\gamma_2 a_2^2\right)}\right)^q\right)\\ &\times\left(1-e^{-\frac{\gamma_2 m_{\tilde{h}_3}\left(\rho\sigma_3^2+1\right)}{\rho\Omega_{\tilde{h}_3}}}\sum_{p=0}^{m_{\tilde{h}_3}-1}\frac{1}{p!}\left(\frac{\gamma_2 m_{\tilde{h}_3}\left(\rho\sigma_3^2+1\right)}{\rho\Omega_{\tilde{h}_3}}\right)^p\right.\\ &\times e^{-\frac{\gamma_2 m_{\tilde{h}_1}\left(\sigma_1^2+1/\rho\right)}{\left(a_1^2-\gamma_2 a_2^2\right)\Omega_{\tilde{h}_1}}}\sum_{k=0}^{m_{\tilde{h}_1}-1}\sum_{n=0}^{k}\binom{k}{n}\frac{\Gamma\left(m_{g_1}+n\right)!\left(\sigma_1^2+1/\rho\right)^{k-n}}{\Gamma\left(m_{g_1}\right)k!\left(\Omega_{g_1}\Omega_{\tilde{h}_1}\right)^{-n}\left(m_{g_1}\Omega_{\tilde{h}_1}\right)^{-m_{g_1}}}\\ &\times\left(\frac{\gamma_2 m_{\tilde{h}_1}}{\left(a_1^2-\gamma_2 a_2^2\right)\Omega_{\tilde{h}_1}}\right)^k\left.\left(m_{g_1}\Omega_{\tilde{h}_1}+\frac{\gamma_2 m_{\tilde{h}_1}\Omega_{g_1}}{\left(a_1^2-\gamma_2 a_2^2\right)}\right)^{-m_{g_1}-n}\right)\end{aligned} \tag{25}$$

3.4. Throughput

Based on achievable outage probability, we can compute throughput as below

$$\mathcal{TP} = (1-\mathcal{OP}_{U_1})R_1 + (1-\mathcal{OP}_{U_2})R_2 \tag{26}$$

4. NUMBER RESULT

In this section, we perform simulations to check the corrections of derived formulas. We set $a_1^2 = 0.8$, $a_2^2 = 0.2$, $R_1 = R_2 = 1$, $\sigma^2 = \sigma_1^2 = \sigma_2^2 = \sigma_3^2 = 0.01$, $m = m_{g_1} = m_{\tilde{h}_1} = m_{\tilde{h}_2} = m_{\tilde{h}_3} = 2$, $\Omega_{\tilde{h}_1} = 2$, $\Omega_{\tilde{h}_2} = \Omega_{\tilde{h}_3} = 1$ and $\Omega_{g_1} = 0.05$.

Figure 2 shows outage performance of user U_1 versus the transmit SNR. We can see FD case exhibits its superiority compared with HD case. At high SNR region, SINR would be better and hence such outage probability can be improved at high SNR. Similar trend can be seen in Figure 3 for case of user U_2. We change value of fading severity parameter m and a gap exists when comparing these cases of m. Similar performance is presented in Figure 4, Figure 5 for user U_1, U_2 respectively for two cases of noise term. Finally, throughput meets highest as SNR is greater than 20 dB shown in Figure 6. The reason is that throughput depends on outage probability.

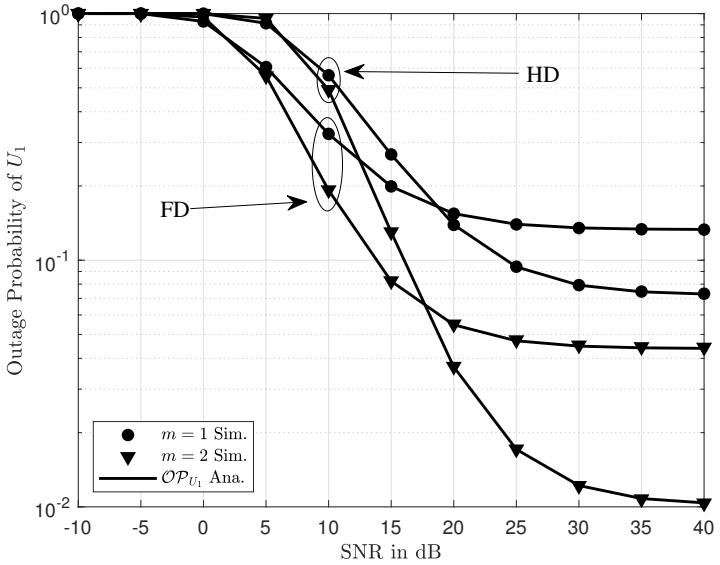

Figure 2. The outage probability of U_1 versus SNR varying m with $\sigma^2 = 0.01$.

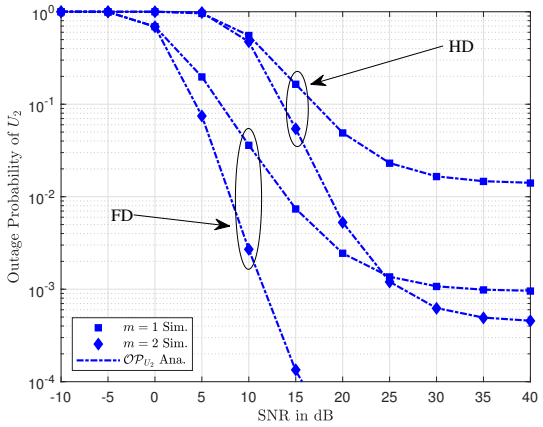

Figure 3. The outage probability of U_2 versus SNR varying σ^2 with $m = 2$.

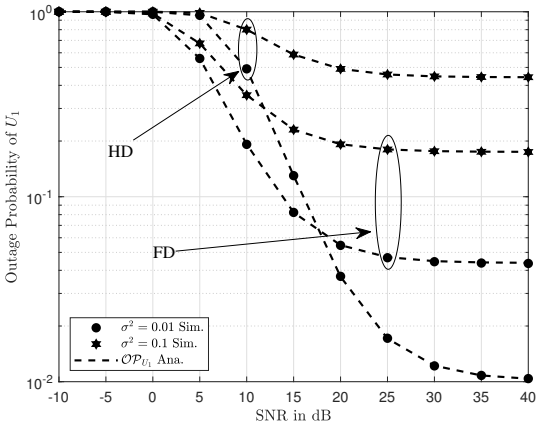

Figure 4. The outage probability of U_1 versus SNR varying m with $\sigma^2 = 0.01$

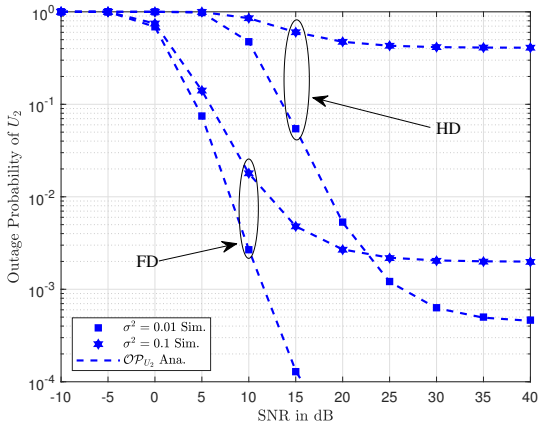

Figure 5. The outage probability of U_2 versus SNR varying σ^2 with $m = 2$

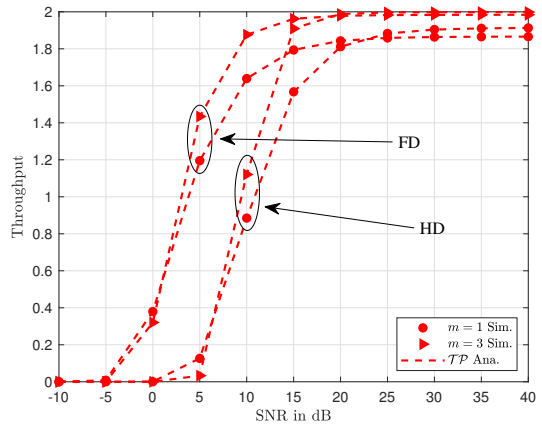

Figure 6. Throughput of system versus SNR varying m with $\sigma^2 = 0.01$

5. CONCLUSION

This paper has studied cooperative NOMA scheme under impact of imperfect CSI. Based on the nature of cooperation, the near user benefits from full-duplex design to serve far user, which improve performance of far user. This results in an enhancement of the downlink NOMA over Nakagami-m fading. We analyze the system outage probability and throughput under different variations of the key system parameters. Finally, simulation results validate our considered system.

REFERENCES

[1] Q. C. Li, H. Niu, A. T. Papathanassiou, and G. Wu, "5G network capacity: Key elements and technologies," *IEEE Veh. Technol. Mag.*, vol. 9, no. 1, pp. 71–78, Mar. 2014.

[2] Y. Saito, A. Benjebbour, Y. Kishiyama, and T. Nakamura, "Systemlevel performance evaluation of downlink non-orthogonal multiple access (NOMA)," in *Proc. IEEE Int. Symp. Pers., Indoor Mobile Radio Commun. (PIMRC)*, Sep. 2013, pp. 611–615.

[3] T. M. Cover and J. A. Thomas, Elements of Information Theory. New York, NY, USA: Wiley, 1991.

[4] Z. Ding, X. Lei, G. K. Karagiannidis, R. Schober, J. Yuan, and V. K. Bhargava, "A survey on nonorthogonal multiple access for 5G networks: Research challenges and future trends," *IEEE J. Sel. Areas Commun.*, vol. 35, no. 10, pp. 2181–2195, Oct. 2017.
[5] Z. Xiang, W. Yang, G. Pan, Y. Cai, and Y. Song, "Physical Layer Security in Cognitive Radio Inspired NOMA Network," *IEEE Journal of Selected Topics in Signal Processing*, vol. 13, no. 3, pp. 700–714, Jun. 2019.
[6] W. Wu, F. Zhou, R. Q. Hu, and B. Wang, "Energy-Efficient Resource Allocation for Secure NOMA-Enabled Mobile Edge Computing Networks," *IEEE Transactions on Communications*, vol. 68, no. 1, pp. 493–505, Jan. 2020.
[7] W. Wu, X. Yin, P. Deng, T. Guo, and B. Wang, "Transceiver Design for Downlink SWIPT NOMA Systems with Cooperative Full-Duplex Relaying," *IEEE Access*, vol. 7, pp. 33 464–33 472, 2019.
[8] F. Zhou, Y. Wu, Y. C. Liang, Z. Li, Y. Wang, and K. K. Wong, "State of the Art, Taxonomy, and Open Issues on Cognitive Radio Networks with NOMA," *IEEE Wireless Communications*, vol. 25, no. 2, pp. 100–108, Apr. 2018.
[9] Z. Ding, L. Dai, and H. V. Poor, "MIMO-NOMA Design for Small Packet Transmission in the Internet of Things," *IEEE Access*, vol. 4, pp. 1393–1405, 2016.
[10] Z. Xiang, W. Yang, Y. Cai, J. Xiong, Z. Ding, and Y. Song, "Secure Transmission in a NOMA Assisted IoT Network with Diversified Communication Requirements," *IEEE Internet of Things Journal*, pp. 1–13, 2020.
[11] M. Shirvanimoghaddam, M. Condoluci, M. Dohler, and S. J. Johnson, "On the Fundamental Limits of Random Non-Orthogonal Multiple Access in Cellular Massive IoT," *IEEE Journal on Selected Areas in Communications*, vol. 35, no. 10, pp. 2238–2252, Oct. 2017.
[12] Y. Song, W. Yang, X. Yang, Z. Xiang, and B. Wang, "Physical Layer Security in Cognitive Millimeter Wave Networks," *IEEE Access*, vol. 7, pp. 109162–109180, 2019.
[13] Y. Song, W. Yang, Z. Xiang, N. Sha, H. Wang, and Y. Yang, "An Analysis on Secure Millimeter Wave NOMA Communications in Cognitive Radio Networks," *IEEE Access*, vol. 8, pp. 78 965–78 978, 2020.
[14] D.-T. Do, A.-T. Le and B.-M. Lee, "On Performance Analysis of Underlay Cognitive Radio-Aware Hybrid OMA/NOMA Networks with Imperfect CSI," *Electronics*, vol. 8 no. 7, p. 819, 2019.
[15] Dinh-Thuan Do, A. Le and B. M. Lee, "NOMA in Cooperative Underlay Cognitive Radio Networks Under Imperfect SIC," *IEEE Access*, vol. 8, pp. 86180-86195, 2020.
[16] M. Alkhawatrah, Y. Gong, G. Chen, S. Lambotharan, and J. A. Chambers, "Buffer-Aided Relay Selection for Cooperative NOMA in the Internet of Things," *IEEE Internet of Things Journal*, vol. 6, no. 3, pp. 5722–5731, Jun. 2019.
[17] D-T. Do, M. V. Nguyen, F. Jameel, R. Jäntti and I. S. Ansari, "Performance Evaluation of Relay-Aided CR-NOMA for Beyond 5G Communications," in *IEEE Access*, vol. 8, pp. 134838-134855, 2020.
[18] D.-T. Do, M.-S. Van Nguyen, T.-A. Hoang and Byung M. Lee, "Exploiting Joint Base Station Equipped Multiple Antenna and Full-Duplex D2D Users in Power Domain Division Based Multiple Access Networks," *Sensors*, vol. 19, no. 11, p. 2475, 2019.
[19] D.-T. Do, A.-T. Le, C.-B. Le and B. M. Lee "On Exact Outage and Throughput Performance of Cognitive Radio based Non-Orthogonal Multiple Access Networks With and Without D2D Link," *Sensors*, vol. 19, no. 15, p.3314, 2019.
[20] D.-T. Do and A.-T. Le, "NOMA based cognitive relaying: Transceiver hardware impairments, relay selection policies and outage performance comparison," *Computer Communications*, Vol. 146, pp. 144-154, 2019.
[21] J. Men, J. Ge, and C. Zhang, "Performance analysis for downlink relaying aided non-orthogonal multiple access networks with imperfect CSI over Nakagami-m fading," *IEEE Access*, vol. 5, pp. 998–1004, 2017.
[22] Z. Ding, Z. Yang, P. Fan, and H. V. Poor, "On the performance of non-orthogonal multiple access in 5G systems with randomly deployed users," *IEEE Signal Process. Lett.*, vol. 21, no. 12, pp. 1501–1505, Dec. 2014.
[23] Z. Ding, P. Fan, and H. V. Poor, "Impact of user pairing on 5G nonorthogonal multiple-access downlink transmissions," *IEEE Trans. Veh. Technol.*, vol. 65, no. 8, pp. 6010–6023, Aug. 2016.
[24] Z. Chen, Z. Ding, X. Dai, and G. K. Karagiannidis, "On the application of quasi-degradation to MISO-NOMA downlink," *IEEE Trans. Signal Process.*, vol. 64, no. 23, pp. 6174–6189, Dec. 2016.
[25] C. Li, Q. Zhang, Q. Li, and J. Qin, "Price-based power allocation for non-orthogonal multiple access systems," *IEEE Wireless Commun. Lett.*, vol. 5, no. 6, pp. 664–667, Dec. 2016.
[26] L. Ma, S. Zhou, G. Qiao, S. Liu, and F. Zhou, "Superposition coding for downlink underwater acoustic OFDM," *IEEE J. Ocean. Eng.*, vol. 42, no. 1, pp. 175–187, Jan. 2017.
[27] X. Ren, M. Tao, and W. Chen, "Compressed channel estimation with position-based ICI elimination for high-mobility SIMO-OFDM systems," *IEEE Trans. Veh. Technol.*, vol. 65, no. 8, pp. 6204–6216, Aug. 2016.
[28] Z. Yang, Z. Ding, P. Fan and G. K. Karagiannidis, "On the Performance of Non-orthogonal Multiple Access Systems With Partial Channel Information," *IEEE Trans. Commun.,* vol. 64, no. 2, pp. 654-667, Feb. 2016.
[29] Xuan-Xinh Nguyen and Dinh-Thuan Do, "System performance of cooperative NOMA with full-duplex relay over nakagami-m fading channels." *Mobile Information Systems*, 2019.
[30] I.S. Gradshteyn and I.M. Ryzhik, Table of integrals, Series, and Products, *7th ed. San Diego, CA, USA: Academic Press,* 2007